



Emittance control in Laser Wakefield Accelerator

S. Cheshkov, T. Tajima, C. Chiu, and F. Breitling

Citation: [AIP Conference Proceedings](#) **569**, 163 (2001); doi: 10.1063/1.1384347

View online: <http://dx.doi.org/10.1063/1.1384347>

View Table of Contents: <http://scitation.aip.org/content/aip/proceeding/aipcp/569?ver=pdfcov>

Published by the [AIP Publishing](#)

Articles you may be interested in

[Table top accelerator with extremely bright beam](#)

AIP Conf. Proc. **569**, 881 (2001); 10.1063/1.1384414

[Demonstration of a laser-driven prebuncher staged with a laser accelerator—the STELLA program](#)

AIP Conf. Proc. **569**, 146 (2001); 10.1063/1.1384345

[GeV laser acceleration research at JAERI-APR](#)

AIP Conf. Proc. **569**, 112 (2001); 10.1063/1.1384341

[Laser-Plasma Accelerators: A status report](#)

AIP Conf. Proc. **569**, 85 (2001); 10.1063/1.1384338

[Summary report of Working Group 2 on laser-plasma acceleration concepts](#)

AIP Conf. Proc. **569**, 35 (2001); 10.1063/1.1384332

Emittance Control in Laser Wakefield Accelerator

S. Cheshkov¹, T. Tajima^{1,2}, C. Chiu¹, F. Breitling¹

¹*Department of Physics, University of Texas at Austin, Austin, TX 78712*

²*Lawrence Livermore National Laboratory, CA 94550*

Abstract. In this paper we summarize our recent effort and results in theoretical study of the emittance issues of multistaged Laser Wakefield Accelerator (LWFA) in TeV energy range. In such an energy regime the luminosity and therefore the emittance requirements become very stringent and tantamount to the success or failure of such an accelerator. The system of such a machine is very sensitive to jitters due to misalignment between the beam and the wakefield. In particular, the effect of jitters in the presence of a strong focusing wakefield and initial longitudinal phase space spread of the beam leads to severe transverse emittance degradation of the beam. To improve the emittance we introduce several methods: a mitigated wakefield focusing by working with a plasma channel, an approximately synchronous acceleration in a superunit setup, the “horn” model based on exactly synchronous acceleration achieved through plasma density variation and lastly an algorithm based on minimization of the final beam emittance to actively control the stage displacement of such an accelerator.

INTRODUCTION

The concept of LWFA was originally proposed by Tajima and Dawson [1]. Since then there has been significant advance in this area. For a review, see Esarey et al [2].

In pursuit of the next energy frontier, a laser-based wakefield linear e^+e^- collider at high energies (such as 5 TeV) has been considered for which many wakefield units are needed to reach the desired energy. However, the high energy is not the only requirement, such a collider demands an extremely small beam emittance and thus extremely precise beam handling. To identify the crucial physical and technological problems associated with this, a systems approach through a dynamical map has been introduced [3–5]. There was also an earlier study on a 5 TeV laser-wakefield collider [6]. Emittance degradation in TeV-accelerators for the case of a full filamentation in the transverse phase space was considered in ref. [7].

In [5], the study of emittance degradation in the presence of jitters, associated with stochastic misalignment between the beam and the wakefields was carried out where the plasma medium is uniform and the beam is accelerated over a full

quarter-wave region. One finds that the system is sensitive to transverse offsets due to the wakefield averaging over the entire accelerating phase and thus typically providing a very strong focusing.

A possible way to decrease the strong focusing wakefield is to use the hollow channel design [8]. A drawback is that due to the finite density gradient near the wall of the cavity, there is a local plasma frequency which would match the wakefield frequency and lead to resonance absorption [9]. In [5], numerical models with beam acceleration over a full quarter-wave-region were considered. These models are for both without involving the plasma channel and with the plasma channel ignoring the resonance absorption effect. The former will be referred to as the CTHY model and the latter the CTHY1 model and are briefly described in Sec.2.

From a general consideration, one expects that the emittance degradation should depend on the phase-range through which the acceleration occurs. Using two different approaches [10,11] we explore ways to improve the resilience against jitters through variations of the loading phase and also of the phase interval of acceleration. Computer simulation indicates that when the acceleration phase is approximately fixed (the phase slip is small) there is an inverse power behavior (for a fixed final energy of the particles), in particular, the emittance degradation decreases like $1/N_T$, where N_T is the total number of acceleration units. This confirms the theoretical expectation of CTHY deduced from a statistical theory [5]. The inverse power law suggested that through the use of small acceleration intervals one may be able to achieve high resilience against jitters. The second approach is to work with a synchronous acceleration model, where there is no phase slip at all. It was pointed out by Katsouleas [12] over a decade ago that synchronous acceleration can be achieved by varying the plasma density. More specifically, consider the case where the local density along the beam direction is gradually increasing. Then the wavelength of the plasma waves, on which the beam electrons are riding, becomes shorter and shorter. If the rate of the phase-slip of the beam electrons exactly matches the rate of the phase advance due to the shrinkage of the plasma waves, a continuous acceleration without any phase-slip may be achieved. From a study on the hydrodynamics of a nozzle flow [13], we find that if there is a steady flow opposite to the direction of the beam propagation, by fine tuning the increase of the nozzle cross section along the beam, one can control the corresponding increase of the plasma density and in turn achieve a synchronous acceleration. Here the acceleration unit has a horn shape and we refer to this model as the “horn model” [11]. Based on the Katsouleas’s matching condition, we have derived a set of analytic expressions which have been incorporated in the dynamical map. Our work [11] also takes into account the conservation of energy in the context of the pump-depletion effect [14] and the adiabatic invariance property throughout the acceleration process [15]. The computer simulations for the horn model with a small loading phase show a definite improvement over CTHY model. Lastly we propose an active alignment control which can significantly reduce the final emittance of the beam as illustrated by our preliminary numerical results. The analysis is done by introducing a feedback in our multistage systems code which adjusts the accelerator stages based on

the calculation of the final emittance only and minimization criteria.

MULTISTAGE ACCELERATION, MAP APPROACH AND EMITTANCE DEGRADATION

In general, TeV center of mass energies of colliding particles require multistage acceleration even if we assume large acceleration gradients typical for the plasma based accelerators. To study such an accelerator system we introduced a map approach described in [3–5]. The longitudinal phase space transformations (for the differential phase $\delta\Psi$ and the differential Lorentz factor $\delta\gamma$, respectively) stage by stage are described by the longitudinal map:

$$\delta\Psi_{n+1} = \delta\Psi_n \quad (1)$$

$$\delta\gamma_{n+1} = 2\gamma_p^2 \Phi_0 (\cos(\Psi_s + \Delta) - \cos \Psi_s) \delta\Psi_n + \delta\gamma_n, \quad (2)$$

where n enumerates the stage, Ψ_s is the “synchronous” or the loading phase, Δ is the phase slippage, γ_p is the Lorentz factor of the plasma wave, and $\Phi_0 \approx a_0^2$, where a_0 is the normalized vector potential of the laser. Characteristic for these equations is that the particles are extremely relativistic ($\gamma \sim 10^5 - 10^7$) so that the synchrotron oscillation frequency approaches zero. Transverse motion is described by the following equation (for each stage, z is defined with respect to the beginning point of this stage along the beam propagation direction)

$$\ddot{\tilde{x}} + \omega_\beta^2 \sin(\omega_s z + \Psi_s + \delta\Psi_n) \tilde{x} = 0, \quad (3)$$

where $\ddot{\tilde{x}} = \frac{d^2 \tilde{x}}{dz^2}$,

$$\omega_s = \frac{k_p}{2\gamma_p^2}, \quad \omega_\beta = \frac{2}{r_s} \left(\frac{\Phi_0}{\gamma} \right)^{1/2}, \quad (4)$$

and $\tilde{x} = \sqrt{\gamma} x$. In Eq. (4), r_s is the laser spot size and k_p is the plasma wavenumber. For analytic solution additional approximations are needed. The analysis here is based on harmonic oscillator model and free drift of the particles between the stages. So the transverse map becomes

$$\begin{pmatrix} \tilde{x}_{n+1} \\ \dot{\tilde{x}}_{n+1} \end{pmatrix} = M_n \begin{pmatrix} \tilde{x}_n \\ \dot{\tilde{x}}_n \end{pmatrix}, \quad (5)$$

$$M_n = \begin{pmatrix} \cos(\omega l), & \frac{1}{\omega} \sin(\omega l) \\ -\omega \sin(\omega l), & \cos(\omega l) \end{pmatrix} \cdot M_{\text{gap}}, \quad M_{\text{gap}} = \begin{pmatrix} 1 & L \\ 0 & 1 \end{pmatrix}, \quad (6)$$

where $l = \Delta/\omega_s$ is the stage length. In Eq. (6), ω is the betatron frequency¹ (in units of 1/m), and M_{gap} is for a free drift space. We have also considered M_{gap} in

¹) In Eq. (6) the betatron frequency ω is defined by $\omega^2 = \omega_\beta^2 \langle \sin \Psi \rangle$, for details, see [11].

which magnets are included [10,11]. Even though our simplified notation in Eq. (6) does not explicitly show it, it is important to remember that the transverse matrix depends on the stage number (since particles are being accelerated and $\omega \propto \frac{1}{\sqrt{\gamma}}$) and also is different for different particles due to the spread in ω which in turn is caused by the particle spread in the longitudinal phase space ($\delta\Psi, \delta\gamma$).

We now introduce errors [5] in the accelerating structure, namely jitter of the aligned wakefield (by whatever mechanism) stage by stage. The result of this is a phase space mixing, which depends on absolute spread of the betatron frequencies and jitter magnitude. It degrades the transverse emittance of the beam. Typical strength of the focusing force is of great importance for the rate at which mixing and correspondingly the emittance degradation takes place. In our model the dislocation of the aligned position of each stage is a stochastic variable with Gaussian distribution of standard deviation $\sigma_{\mathcal{D}}$. The transverse map is modified according to

$$\begin{pmatrix} \tilde{x}_{n+1} \\ \dot{\tilde{x}}_{n+1} \end{pmatrix} = M_n \begin{pmatrix} \tilde{x}_n - \tilde{\mathcal{D}}_n \\ \dot{\tilde{x}}_n \end{pmatrix} + \begin{pmatrix} \tilde{\mathcal{D}}_n \\ 0 \end{pmatrix} \quad (7)$$

where \mathcal{D}_n is the misalignment of stage n . The total transverse map after N stages becomes

$$\begin{aligned} \begin{pmatrix} \tilde{x}_{N+1} \\ \dot{\tilde{x}}_{N+1} \end{pmatrix} &= M_N M_{N-1} \dots M_2 (1 - M_1) \begin{pmatrix} \tilde{\mathcal{D}}_1 \\ 0 \end{pmatrix} + \dots (1 - M_N) \begin{pmatrix} \tilde{\mathcal{D}}_N \\ 0 \end{pmatrix} \\ &+ M_N M_{N-1} \dots M_1 \begin{pmatrix} \tilde{x}_1 \\ \dot{\tilde{x}}_1 \end{pmatrix} \end{aligned} \quad (8)$$

The stochastic map (8) leads to a transverse emittance degradation. Computer simulation with small random dislocations of magnitude $\sigma_{\mathcal{D}} = 1 \cdot 10^{-7}$ m is presented in Figure 1a and Figure 1c [4]. We see that in this case (corresponds to design I in [6]) we have a severe emittance growth (the initial normalized emittance is 2.2 nm). Additional results can be found in [3–5]. In general, the problem can be cured by decreasing the focusing of the accelerator system. One possible way is to use a plasma channel [8,9]. It provides a linear weak focusing and we showed in [4] that its performance in a collider application is promising.

A detailed study of the map and emittance degradation properties can be found in [5]. In the limit of small betatron frequency ω , namely $\omega l < 1$ and small distance between the stages and in fixed energy approximation the emittance growth after N stages as shown in [5] is:

$$\Delta\epsilon \approx \frac{1}{2} \gamma \omega (\omega l)^2 \sigma_{\mathcal{D}}^2 N . \quad (9)$$

The alignment errors introduce randomness in the phase space particle positions upon reentry to the next stage, the differential betatron oscillations mix these positions causing an emittance growth. This is valid in the case of a small drift

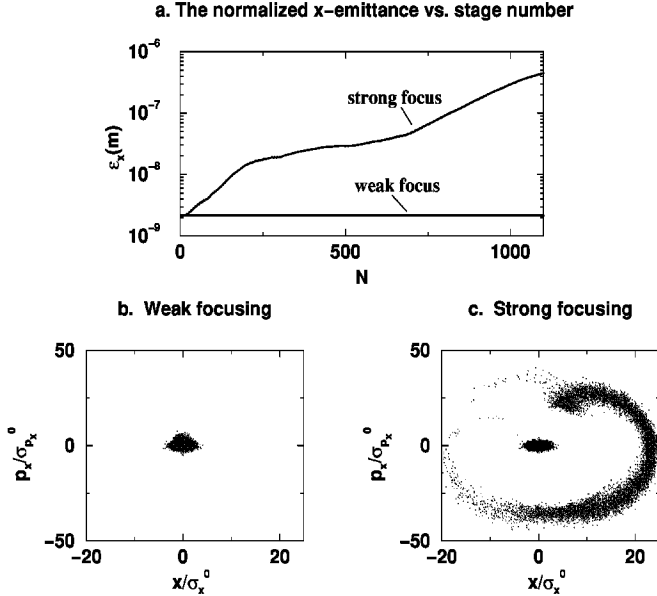


FIGURE 1. The normalized x-emittance vs. stage number and the transverse phase space before and after the acceleration to 2.5 TeV for weak and strong wakefield properties. Parameters for the CTHY model, i.e. the strong focusing case (uniform plasma) are $\gamma_p = 100$, $L = 15$ cm, $\epsilon_x^0 = 2.2$ nm, $r_s = 0.5$ mm, $a_0 = 0.5$, dislocation size = $0.1 \mu\text{m}$, $\sigma_\gamma/\gamma = 0.01$, $\sigma_\Psi = 0.01$. Parameters used for the CTHY1 model, i.e. the weak focusing (plasma channel) are given in Sec. 2

$L \ll l$. If this is not the case, but $L\omega \ll 1$ is still satisfied we can modify the above equation by introducing $\omega' = \omega\sqrt{l/(l+L)}$. Then the betatron phase advance per stage (wakefield and drift) is given by $\omega'(l+L)$ and in all formulas ω should be replaced by ω' and l by $l+L$.

Since the energy increases Eq. (9) needs to be further modified. Denote the Lorenz factor increase per stage by $\Delta\gamma$. In the adiabatic limit we obtain

$$\Delta\epsilon \approx \frac{1}{2}\gamma\omega(\omega l)^2\sigma_D^2 \left(\frac{\gamma}{\Delta\gamma}\right)^{1/2} \sqrt{N \ln\left(1 + \frac{\Delta\gamma N}{\gamma}\right)}, \quad (10)$$

where now γ is the initial particle Lorenz factor and ω is the initial betatron frequency. Typically $\Delta\gamma \approx \frac{ea_0^2 E_0 l}{mc^2} = a_0^2 k_p l$, where E_0 is the nonrelativistic wavebreaking field, and $\omega \propto \frac{a_0}{r_s \sqrt{\gamma}} < \sin\Psi >^{1/2}$, so we obtain

$$\Delta\epsilon \propto \frac{l^{3/2} a_0^2 \sigma_D^2}{r_s^3 k_p^{1/2}} \sqrt{N \ln\left(1 + \frac{\Delta\gamma N}{\gamma}\right)} < \sin\Psi >^{3/2}. \quad (11)$$

A very important result is the strong dependence of the emittance growth on the magnitude of the betatron frequency (or wakefield curvature). Of course, better

control of the errors reduces the emittance degradation. We can also see from Eq. (11) that for a fixed final energy reducing the length of a single stage decreases the emittance growth. This point is exploited in the next section. Scalings of the emittance growth with various parameters can be found in [5]. When the number of stages is relatively small and the phase space mixing is not complete, numerical results appear to be the only reliable way to analyze the properties of the map, analytical estimations are rather difficult. Analytical estimations of emittance growth due to stage misalignment valid in the case of full filamentation (phase space mixing) in a single stage can be found in [7]. In this limit (corresponds to a very strong focusing of the wakefield), control over the emittance growth can be achieved only by precise handling of the beam (namely error control better than the beam size). The results in this limit are reproduced in our theory by replacing the factor ωl in Eq. (9) by unity.

From the computer simulations for the small emittance design [6] for a multi TeV collider we see that in the case of an initially homogeneous plasma it is difficult to avoid a severe emittance growth of the accelerated beam in the presence of small alignment errors stage-by-stage based on reasonable parameters (laser spot size, dislocation size and number of stages). The difficulty is primarily due to the fact that the wakefield focusing too strong in this case. The above considerations do not include the transverse nonlinear effects which also contribute to the emittance increase.

A possible way to decrease the focusing is the “hollow channel” design proposed by [8] in which a preformed vacuum channel in an underdense plasma is discussed. This case offers several important advantages: the focusing force is almost exactly linear and weak in the channel (the weak focusing is a very important improvement over that of a uniform plasma case); there exists a stable propagation solution for the laser mode; the acceleration gradient is very uniform in transverse coordinates within the channel. A drawback is the loss in the magnitude of the accelerating field. The equations for the wakefield in the channel can be found in [8]. There are no major changes to our previous map scheme, there is a reduction in Φ_0 and the magnitude of the focusing changes:

$$\omega_\beta = \frac{k_{ch}}{\sqrt{2}\gamma_p} \left(\frac{\Phi_0}{\gamma} \right)^{1/2},$$

where k_{ch} is the wake wavenumber. Since the γ_p factor is usually large the magnitude of the focusing force decreases significantly. Run shown on Figure 1a and Figure 1b [4] indicates a significant improvement over the previous design. Here we are able to preserve even design I [6] normalized emittance of 2.2 nm. The parameters of the CTHY1 model are: $\gamma_p = 150$, the channel radius $a = 30\mu\text{m}$, the laser spot size $r_s = 50\mu\text{m}$, the plasma density (outside the channel) $n = 5 \cdot 10^{16}\text{cm}^{-3}$, the laser wavelength $\lambda \approx 1\mu\text{m}$, and the drift space of 0.3 m. The magnitude of the stage dislocations is increased to $\sigma_{\mathcal{D}} = 0.5\mu\text{m}$. The remaining parameters are the

same as in the CTHY case. From the graphs we see that the emittance growth of the accelerated beam is now practically negligible and the design is more promising. Unfortunately, there is an additional effect: because in reality we have a finite density gradient it leads to a resonant absorption where the local plasma frequency matches the wakefield frequency. This effect has been studied in [9], where an expression for the quality factor of the hollow channel is derived. Possible low values of this factor limit the acceleration of multiple bunches in a single shot created wakefield. Another way to decrease the wakefield curvature is through the use of transversely shaped laser pulses. A “flat top” laser pulse would produce a small curvature wakefield and correspondingly small focusing force. Creation and propagation of such pulses needs to be studied. In the case of PWFA the density shaping of the driver electron bunch can be achieved by using octuple magnets. Lastly we note that in the weak focusing cases achieved in plasma the collision-induced emittance degradation becomes important, since it is inversely proportional to the betatron frequency. Correspondingly, there is an optimal wakefield focal strength. We will present the results on this in a follow-up paper.

DESIGN ISSUES, APPROXIMATELY SYNCHRONOUS ACCELERATION, HORN MODEL

Accelerator with superunits, chips and magnets

For a fixed final energy it is advantageous [10,11] to increase the number of acceleration stages to have better control of the emittance. See Figure 2. In such scenario of having a very large number of stages, each stage becomes very short (e.g. of the order of 1 cm) and we are led to consider a superunit which is made out of many short tubes or chips, the wakefield within each chip is created by an independent laser pulse. We consider distances of the order of 1m between adjacent superunits to allow the experimental set up needed to maintain superunits including magnets placed over a certain period of length to ensure the quality of the beam. We have considered an illustrative system:

- Total energy: 2.5 TeV, which is used as each of the two arms of the 5 TeV collider. The acceleration is from 0.5 TeV to 2.5 TeV.
- Total number of superunits (SU): 500
- Within one super-unit (SU) there are:
 - 100 stages per SU, and
 - gap = tube = 0.83 cm.
- There is a large-gap between two adjacent super-units: 1m
- Length of the accelerator: about 1300 m.

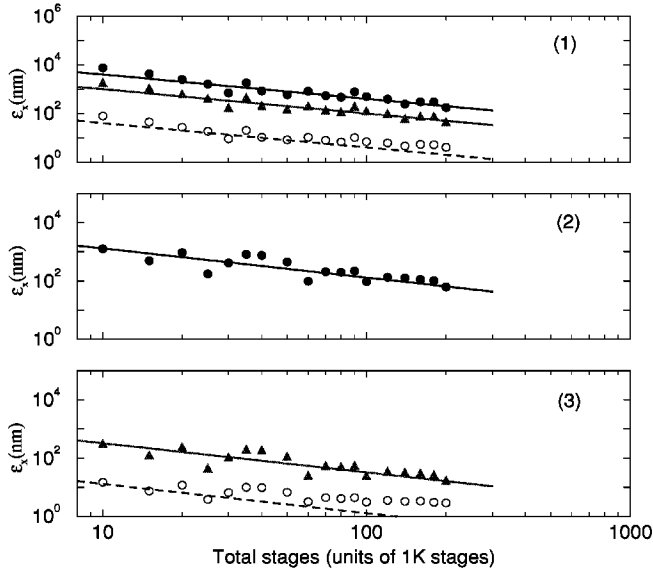


FIGURE 2. Multistages [11]: (1) Gap=10 tubes, $\sigma_D=1, 0.5, \& 0.1 \mu\text{m}$, (2) Gap=tube, $\sigma_D=1 \mu\text{m}$, (3) Gap=tube, $\sigma_D=0.5 \& 0.1 \mu\text{m}$. Each case is compared with the inverse power law $1/N_T$. N_T is the total number of stages.

We proceed to look at how emittance degradation varies as a function of the loading phase for the system of superunits with chips. From Eq. (9) one expects in some average sense

$$\epsilon \propto \omega^3 \propto (\sin \Psi_m)^{3/2}, \quad (12)$$

where Ψ_m is the mean phase of the beam, taken to be $\Psi_m = \Psi_s + 0.5\Delta$. Here Ψ_s is the loading phase and Δ the total phase slip. This implies that the resilience of the present system against jitters can be further improved, at least in the small loading phase region, by lowering the loading phase value. We consider two loading phases, i.e. $\Psi_s = 0.15$ rad and $\Psi_s = 0.05$ rad. Figure 3 (taken from [11]) shows the interim emittance degradation for three cases. There are 50K stages and all cases are at the final energy of 2.5 TeV. The stochastic theory if applicable implies that the intermediate emittance should grow approximately² linearly with the number of stages. Approximate mean linear behavior is observed for curves a and b. For curve c, there is a rapid rise up to about 20% of the total stages, which is followed by an approximately linear mean behavior. To conclude, within the present chip-model the final emittance has been reduced to say less than

²) This approximate linearity is valid as is Eq. (9) only under assumption of a constant typical energy beam transport. Obviously, the linearity is not a good approximation for very large N , when the asymptotic behavior is $\Delta\epsilon \propto \sqrt{N \ln N}$ as seen from Eq. (11)

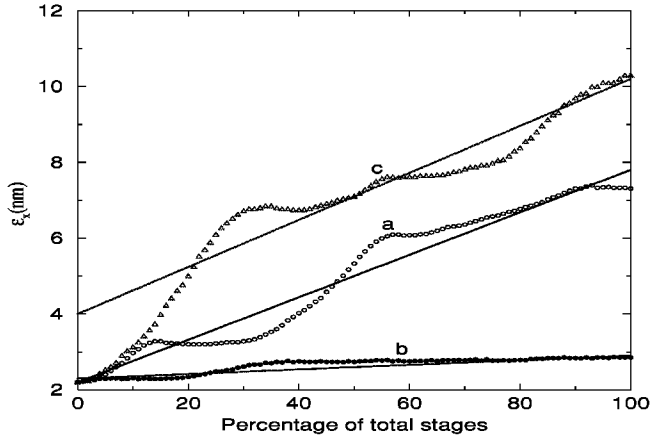


FIGURE 3. The interim emittance degradation behavior as the beam particles traverse through the system of a chip model for $\sigma_D = 0.1\mu\text{m}$. For each case, a solid line of a linear behavior is included to guide the eyes.

Curve a: Total stages: 50K, $\Psi_s = 0.15$ rad.

Curve b: Total stages: 50K, $\Psi_s = 0.05$ rad.

Curve c: Total stages: 20K, $\Psi_s = 0.05$ rad.

$2\epsilon_0$, where ϵ_0 is the initial normalized transverse emittance of 2.2nm . This is to be compared to the situation in the CTHY model, where the final emittance is beyond $100\epsilon_0$. This, however, is at the expense of introducing 50 times more laser pulses, which increases the power consumption by many folds. Thus it has severe practical limitations. These limitations might be ameliorated by adopting a technique to flip a phase by π by introducing two counterpropagating lasers with slightly different colors (G. Shvets' method [16]).

Synchronous Acceleration

As mentioned earlier for the “horn model” [11], synchronous acceleration may be achieved through a specific variation of the plasma density [12]. Consider a steady adiabatic flow of a fluid from a reservoir through a nozzle say in the z direction. Let the static fluid density of the fluid in the reservoir be ρ_0 , which will be referred to as the quiescent density. Denote the fluid density at z along the nozzle be $\rho(z)$. In the [11] we showed that based on fluid dynamics [13] the following relation is valid:

$$A(z) = \text{const} \left(\frac{\rho(z)}{\rho_0} \right) \sqrt{1 - \left(\frac{\rho(z)}{\rho_0} \right)^{\gamma-1}}, \quad (13)$$

where γ is the usual ratio of the specific heat at a constant pressure to that at a constant volume. The region of interest is characterized by a subsonic fluid flow

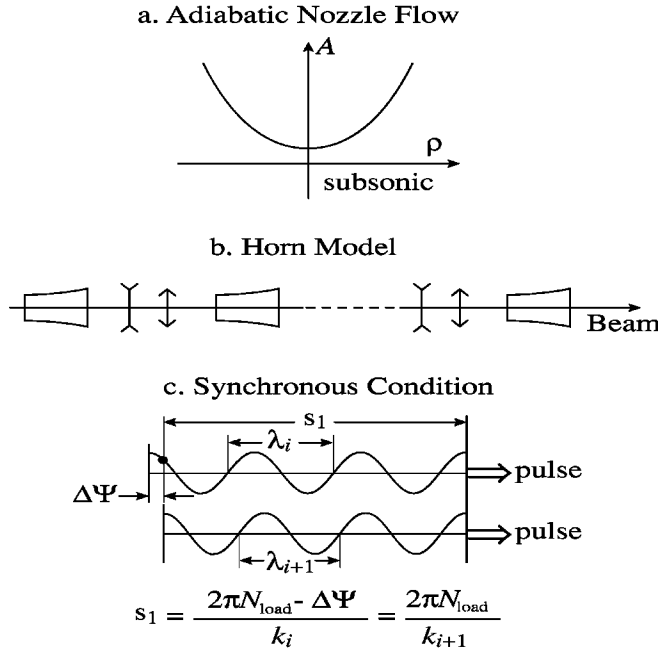


FIGURE 4. The Horn model and the matching condition

(see Figure 4a), where there is a one-to-one relationship between the cross sectional area A , and the plasma density ρ . By increasing the cross section along the beam direction in a specified way one may achieve the required density function. Looking down the stream of the beam, the accelerator consists of a system of aligned horns, although in some cases the increase in radius may be slight. This is the reason why we refer to the present model as the “horn model”. See Figure 4b. We now come to Katsouleas’s matching condition, see Figure 4c. Consider the wakefield acceleration of a beam electron which is located at the center of the beam. Let the “loading number” N_{load} be the number of wave crests the electron is lagging behind the laser pulse. If the initial electron phase relative to the local wakefield, as defined earlier, is Ψ_s , then the electron phase relative to the laser pulse defined by the local plasma wave number k_p is

$$k_p s_1 = 2\pi N_{load} - \Psi_s,$$

where s_1 is the distance from the electron to the pulse measured in the rest frame of the pulse. To motivate the matching condition, for the time being imagine the horn has been divided into many segments. We will assume that the density is constant within each segment. For the i th and the $i+1$ th segments, the wave numbers are k_{pi} and k_{pi+1} , respectively. The i th segment has a width Δz and has a phase-slip $\Delta\Psi$. Here its phase relative to the pulse measured by the wave number of the i th segment

is $k_{pi}s_1 = 2\pi N_{load} - \Psi_s - \Delta\Psi$. The synchronous condition requires the recovery of the initial phase at the start of the $i+1$ th segment, i.e. $k_{pi+1}s_1 = 2\pi N_{load} - \Psi_s$. In other words, the matching condition is given by

$$\frac{2\pi N_{load} - \Psi_s - \Delta\Psi}{k_{pi}} = \frac{2\pi N_{load} - \Psi_s}{k_{pi+1}}. \quad (14)$$

We write $k_{pi+1} = k_{pi} + \frac{dk}{dz}\Delta z$, where Δz is the width of the i th segment. In the continuum limit, after some algebra it leads to

$$\frac{1}{k_p} \cdot \frac{dk_p}{dz} = \frac{1}{(2\pi N_{load} - \Psi_s)} \cdot \frac{d\Psi}{dz} = \frac{1}{2(2\pi N_{load} - \Psi_s)c} \cdot \frac{\omega_p^3}{\omega_0^2}. \quad (15)$$

The first equality is the Katsouleas' condition for synchronous acceleration. The frequency of the laser pulse is denoted by ω_0 . To evaluate the number density variation within the horn, we first recall that the frequency of plasma waves is proportional to the square-root of the number density. Thus the z -dependence of all three quantities: the number density of the plasma medium, the frequency and the wave number of plasma waves, may be specified by a single z -dependent function $\zeta(z)$. In particular, one may write

$$n(z) = n_0\zeta(z)^2, \quad \omega_p(z) = \omega_{p0}\zeta(z), \quad \text{and} \quad k_p(z) = k_{p0}\zeta(z), \quad (16)$$

Substituting Eq.(16) into Eq.(15) gives

$$\frac{1}{k} \cdot \frac{dk}{dz} = \frac{1}{\zeta} \cdot \frac{d\zeta}{dz} = \frac{1}{2(2\pi N_{load} - \Psi_s)c} \cdot \frac{\omega_{p0}^3}{\omega_0^2} \zeta^3, \quad (17)$$

To the extent one neglects the pump-depletion effect [14], i.e. the loss of laser pulse energy as it traverses through the horn, the intensity and the frequency of the laser pulse is assumed to be constant. Integrating over Eq. (17) leads to

$$\zeta(z) = \frac{1}{(1 - z/z_0)^{1/3}}, \quad \text{with} \quad z_0 = \frac{2(2\pi N_{load} - \Psi_s)c}{3} \cdot \frac{\omega_0^2}{\omega_{p0}^3}. \quad (18)$$

In a similar fashion pump depletion effect and the adiabatic invariance can be included in our scheme, however it involves significant amount of algebra and is left for [11]. All this leads to modifications in the longitudinal and transverse transfer map. Here we discuss only the numerical results. For the present synchronous acceleration case, there is no quarter-wavelength restriction, so the tube length can *a priori* vary over a range of values. We have verified that the emittance degradation is also not too sensitive to the loading number. Here is an illustrative case [11]. The tube length is 0.35m and the loading number is 5. The density variation per horn is 7%, with the acceleration energy per stage 2.08 GeV, which is comparable to that of the CTHY model. In Figure 5 [11], curve-a corresponds to the case where

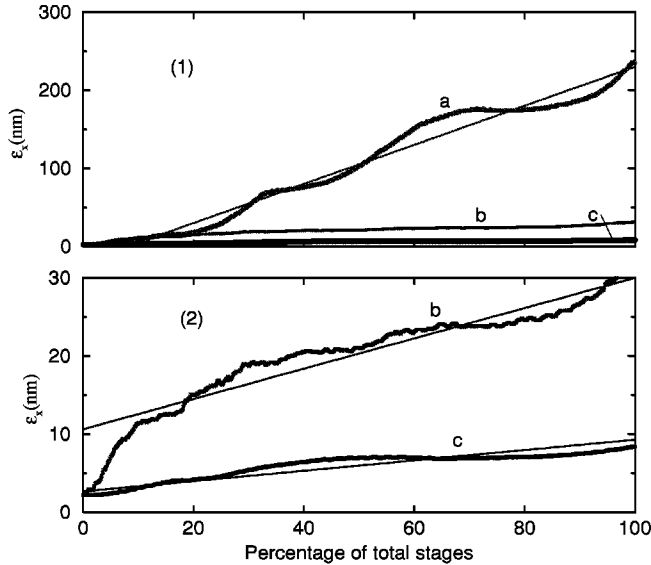


FIGURE 5. The emittance degradation for three cases of the horn model.

Curve-a: $\Psi = 0.15$ rad

Curve-b: $\Psi = 0.04$ rad

Curve-c: $\Psi = 0.04$ rad and $\sigma_\psi = 0.0001$ rad

$\Psi_s = 0.15$ rad. Here the final emittance is $\epsilon = 237\text{nm} \sim 108\epsilon_0$, which is in the same ballpark as that of the CTHY model. So far we have not gained much ground. The important case is curve-b, which is the case where $\Psi_s = 0.04$ rad. It has a final emittance $\epsilon = 31.7\text{nm} \sim 14.5\epsilon_0$, which is about an order of magnitude reduction compared to that of the CTHY model. The interim emittance for this case [11] is shown in Figure 5-1 and with an amplified scale in Figure 5-2. The emittance degradation is sensitive to the longitudinal phase spread of the beam which for all cases considered up to now has been taken to be $\sigma_\psi = 0.01$ rad. Curve-c illustrates the case for a negligibly small value of the spread, i.e. $\sigma_\psi = 0.0001$ rad. Here the final emittance is given by $\epsilon = 8.4\text{nm} \sim 3.8\epsilon_0$. See [11] for more details.

EMITTANCE MINIMIZATION CONTROL OF LWFA

In this section we describe preliminary results of our studies on active feedback [17] (and feed forward) control of beams of the LWFA based collider. In the past we introduced the feedforward control of laser optics by the neural net in order to minimize the jitter of the mirror positions [18]. The idea here is to correct the stage positions based on the measurements of the final emittance only rather than to “measure” more difficult quantities of the beam. This is the entropy minimization strategy. We implemented this strategy in our model CTHY. In our computer

code, each transverse stage displacement consists of two parts: constant (in time), with a magnitude in the micron range and random (in time), with a magnitude in the submicron range. After each shot a stage is moved transversely by a certain fraction of a micron. If the emittance is decreased the new position is accepted otherwise the previous position is reset. As a result the emittance can be significantly reduced if the stochastic (in time) jitter is not very large. Typical runs are shown in Figure 6. However, there are several problems: after adjustments the stages are still misaligned (the algorithm finds local minima of the emittance) and correspondingly the beam centroid is usually kicked too much, this method reduces the emittance by a large factor when the emittance growth is large but does not work that well for smaller emittance growth. As a future plan we want to incorporate the beam centroid position in the algorithm and also study the efficacy of the algorithm in different accelerator scenarios.

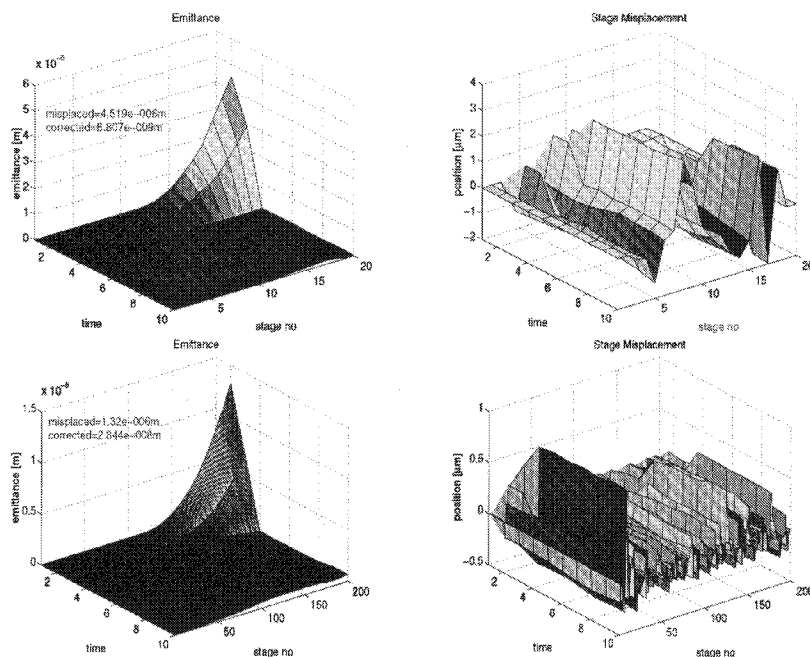


FIGURE 6. The improved control of emittance by feedback control to minimize beam entropy (final emittance). The transverse normalized emittance and stage positions in 20 (upper row) and 200 (lower row) stage units. Magnitude of the constant in time misalignment is $2\mu\text{m}$ and of the stochastic one is $0.1\mu\text{m}$

CONCLUSIONS

Emittance control in a high energy accelerator is of crucial importance. In previous work we identified main effects that degrade the emittance of the beam in

plasma wakefield based collider. In this paper we considered various methods for emittance control and discussed their efficacy and applicability.

ACKNOWLEDGMENT

We thank Mike Downer and also his Femtosecond Spectroscopy Group, especially Andy Rundquist and Erhard Gaul for valuable discussions. We also thank Boris Breizman for discussions on fluid dynamics related issues. This work is supported in part by the US Department of Energy (DOE) and Japan Atomic Energy Research Institute (JAERI). One of us (TT) is also supported in part through a US DOE contract to LLNL, W-7405-Eng.48.

REFERENCES

1. Tajima, T., and Dawson, J., *Phys. Rev. Lett.* **43**, 267 (1979).
2. Esarey, E., Sprangle, P., Krall J., and Ting, A., *IEEE Trans. Plasma Sci.* **24**, 252 (1996).
3. Tajima, T., Cheshkov, S., Horton, W., and Yokoya, K., in *Advanced Accelerator Concepts 8*, edited by W. Lawson, (AIP, New York, 1999), p.153.
4. Cheshkov, S., Tajima, T., Horton, W., and Yokoya, K., in *Advanced Accelerator Concepts 8*, edited by W. Lawson, (AIP, New York 1999), p.343.
5. Cheshkov, S., Tajima, T., Horton, W., and Yokoya, K. accepted to *Phys. Rev. ST Accel. Beams*.
6. Xie, M., Tajima, T., Yokoya, K., and Chattopadhyay, S., in *Advanced Accelerator Concepts 7*, edited by S. Chattopadhyay, (AIP, New York, 1997), p.233.
7. Assmann, R., and Yokoya, K., *Nucl. Instrum. & Methods. A* **410**, 544 (1998).
8. Chiou, T., Katsouleas, T., Decker, C., Mori, W., Wurtele, J., Shvets, G., and Su, J., *Phys. Plasmas* **2**, 310 (1995).
9. Shvets, G., Wurtele, J., Chiou, T., and Katsouleas, T., *IEEE Trans. Plasma Science* **24**, 351 (1996).
10. Chiu, C., Cheshkov, S., and Tajima, T., *Beam Dynamics Newsletter*, **21**, 110 (2000).
11. Chiu, C., Cheshkov, S., and Tajima, T., submitted to *Phys. Rev. ST Accel. Beams*.
12. Katsouleas, T., *Phys. Rev. A* **33**, 2056 (1986).
13. Landau, L., and Lifshitz, E., *Fluid Mechanics*, Pergamon Press, 2d Ed., 1987, Sec. 83 and Sec. 97.
14. Horton, W., and Tajima, T., *Phys. Rev. A* **34**, 4110 (1986).
15. Kuehl, H., Zhang, C., and Katsouleas, T., *Phys. Rev. E* **47**, 1249 (1993).
16. Shvets, G., Fisch, N., Pukhov, A., and Meyer-ter-Vehn, J., *Phys. Rev. E.* **60**, 2218 (1999).
17. Seeman, J. et al. *SLAC-PUB-5439* (1991), and references therein.
18. Breitling, F., Weigel, R., Downer, M., and Tajima, T., submitted to *Rev. Sci. Instrum.*